EFFECTS OF COASTAL ACIDIFICATION ON JAMAICA BAY SALT MARSH NUTRIENT CYCLING

A Final Report of the Tibor T. Polgar Fellowship Program

Beryl C.M. Kahn

Polgar Fellow

Dept. of Biology
The Graduate Center, City University of New York
New York, NY 10016

Project Advisor:

Chester B. Zarnoch
Dept. of Natural Sciences
Baruch College
New York, NY 10010

Kahn, B.C.M., and C.B. Zarnoch. 2022. Effects of Coastal Acidification on Jamaica Bay Salt Marsh Nutrient Cycling. Section VI1-50 pp. *In* D.J. Yozzo, S.H. Fernald, and H. Andreyko (eds.), Final Reports of the Tibor T. Polgar Fellowship Program, 2021. Hudson River Foundation.

ABSTRACT

Nitrogen (N)-loading contributes to coastal habitat degradation through hypoxia and harmful algal blooms. In urbanized estuaries, respiration and decomposition of macroalgal blooms lower seawater pH on a diel/seasonal basis, a process known as coastal acidification. High inputs of labile carbon (C) in the form of macroalgal biomass have been observed in other studies to accelerate decomposition of recalcitrant plant litter, contributing to loss of blue C stocks in seagrass beds. It is unclear how acidification and macroalgal blooms affect nutrient cycling and decomposition, respectively, in urban salt marshes. In this study, nutrient cycling response to manipulated pH was measured in sediment cores collected from two Jamaica Bay salt marsh sites (a restored marsh and a natural, degraded marsh). Decomposition rates of labile vs. recalcitrant litter material were assessed in both marsh sites using tea litterbags. A significant difference in N or oxygen fluxes between ambient-pH and acidified treatments was not observed at either site. This may be due to macroalgal accumulation altering microbial assemblages as well as sediment oxygen conditions. Denitrification and ammonium efflux were higher in the restored marsh than the natural marsh, likely due to the availability of sediment oxygen and organic C. Recalcitrant tea material did not decompose more rapidly in the presence of labile tea material in natural-marsh sediments. Instead, recalcitrant-only material appeared to have a higher decomposition rate than recalcitrant-combined material in the degraded marsh. Understanding the connections between macroalgal blooms and ecosystem processes can inform management and restoration efforts to improve urban marsh habitats.

TABLE OF CONTENTS

LIST OF FIGURES AND TABLES

INTRODUCTION

Coastal habitat decline has long been associated with human activities, particularly as a result of heavy nitrogen (N) inputs from agriculture and wastewater (Howarth and Marino 2006). N-loading has been implicated in stimulating algal blooms, with harmful impacts to marine and estuarine ecosystems. Blooms may lead to high turbidity, which blocks access to sunlight for keystone marine plant species such as seagrasses (Gobler and Sunda 2012). Once these blooms collapse, the decomposition of excess algal biomass by microbial activity depletes coastal waters of oxygen, creating hypoxic conditions that are often deadly to local fish and invertebrate populations (Rabalais et al. 2002).

Microbial decomposition of macro- and microalgae also releases carbon dioxide (CO_2), which reacts with water to form carbonic acid, a weak acid that dissociates further into bicarbonate (HCO_3^-), carbonate (CO_3^{2-}), and hydrogen ions (H^+). The influx of H^+ ions causes local seawater pH to decline, resulting in acidified conditions that correlate with seasonal and diel patterns of algal respiration and decomposition (Wallace et al. 2014). This process is known as coastal acidification. Acidified conditions can be harmful to economically important species such as fish and blue crabs, particularly in their juvenile stages (Wallace and Gobler 2015; Tomasetti et al. 2021).

Seasonal and diel patterns of coastal acidification have been observed in eutrophic estuaries adjacent to areas of high human population density along the Northeast coast of the United States, including New York City's Jamaica Bay (Wallace et al. 2014). Salt marshes in these areas have experienced high levels of loss that may be attributed to eutrophication (Deegan et al. 2012; Day et al. 2018). High N inputs enhance growth of

aboveground biomass in salt marsh grasses at the expense of investment in root growth (Alldred et al. 2017). Consequently, marsh bank structures weaken under N-loading, leading to their collapse (Deegan et al. 2012; Wigand et al. 2014). Coastal acidification may also play a role in marsh loss by altering biogeochemical processes.

Within the Jamaica Bay salt marsh system, declines in pH correlate strongly with abundant growth of macroalgae such as species in the *Ulva* genus, which produce dense biomass around salt marsh islands (NYCDEP 1996; Wallace and Gobler 2015; Lamb 2018). Because high *Ulva* concentration around marsh islands corresponds with pH declines, it has been questioned as to whether changes in pH alter important ecosystem processes in marshes. For example, acidification may change a marsh's ability to remove reactive N, and thereby perpetuate eutrophication-induced erosion in certain marsh areas, and the algal blooms that lead to acidic conditions may change a marsh's ability to store C and accelerate decomposition of existing marsh structure.

Under ambient (non-acidified) conditions, there are several processes that biologically reactive N can undergo in estuarine sediments (Boynton and Kemp 1985). Ammonium (NH_4^+) can be oxidized to form nitrate (NO_3^-), through a process known as nitrification. The NO3- can then be removed from the system through a process known as denitrification, wherein NO_3^- undergoes a series of reductions to N_2 gas under anoxic conditions (Galloway et al. 2003). Conversely, NO_3^- could get recycled to NH_4^+ through a process known as dissimilatory reduction of nitrate to ammonium (DNRA) (Galloway et al. 2003).

Denitrification is usually the dominant N-transformation process in salt marsh sediments (Wigand et al. 2014). Therefore, in eutrophic systems such as Jamaica Bay, a

high denitrification rate can serve as a valuable ecosystem service (Rosenzweig et al. 2018). However, environmental conditions such as organic C availability, hydrogen sulfide (H_2S) concentrations, and NO_3^- levels may change to favor DNRA over denitrification, and can perpetuate N-loaded conditions (Giblin et al. 2013). The relationship between acidification and nutrient cycling remains unclear.

Lower pH may alter microbial community composition as some nitrifying organisms such as ammonia-oxidizing archaea (AOA) prefer low pH, but other nitrifiers such as ammonia-oxidizing bacteria (AOB) are negatively affected by low pH (Yao et al. 2011). The effects of pH-induced changes in community composition on actual nitrification rates are not fully understood, and responses may vary based on specific site conditions such as salinity (Fulweiler et al. 2011). Inorganic C fertilization from respiration may also stimulate nitrification, since nitrifiers are autotrophic (Hutchins et al. 2009). Because denitrifying organisms are NO_3^- limited (Seitzinger et al. 2006), enhanced nitrification may in turn increase denitrification. Similarly, anoxic conditions in salt marsh and eelgrass sediments and those brought about by increased respiration/ decomposition may promote denitrification (Zarnoch et al. 2017; Zhu et al. 2019).

Ulva growth may also impact bank collapse and carbon sequestration in marshes. C-loading from macroalgal accumulation may influence decomposition and C sequestration processes at the marsh edge. Salt marshes are typically known for their capacity for storing blue C, or C that is sequestered by aquatic habitats (Radabaugh et al. 2018). However, *Ulva* accumulation provides an ample stock of labile C which is readily metabolized by abundant microbial activity, which could also accelerate decomposition of recalcitrant C in the form of salt marsh grasses such as *Spartina alterniflora.* Rapid

consumption of both labile and recalcitrant C forms, a process known as cometabolism, is believed to accelerate decomposition of organic matter and inhibit blue C sequestration (Liu et al. 2020).

Sequestered C plays a key role in sediment nutrient cycling processes, although these may differ based on disturbance history of a site (Craft et al. 2003). In natural marsh sites that have experienced little disturbance, organic matter accumulation and C stocks are higher than those that have been restored, with implications for N-cycling (Craft et al. 2003; Alldred et al. 2020). For example, when a large quantity of higher-quality labile C is present, DNRA may be favored, thereby perpetuating eutrophic conditions (Giblin et al. 2013; Murphy et al. 2016). Similarly, C-loading, such as buildup of plant detritus, encourages sulfate-fixing microbes to proliferate, leading to higher efflux of hydrogen sulfide (H_2S) (Rysgaard et al. 1996). Elevated H_2S creates conditions that may also enhance N recycling through DNRA (Brigolin et al. 2021). Therefore, disparities in existing C stocks between restored and natural marsh types may lead to different biogeochemical responses to the acidified conditions present during an *Ulva* bloom, but this has not yet been studied.

In this work, the impact of coastal acidification on salt marsh N-cycling dynamics was explored at a restored marsh (Elders East) and a natural, degrading marsh (Black Bank) in Jamaica Bay, New York, USA. The influence of cometabolism on salt marsh decomposition processes was investigated in these two sites, both of which experience seasonal *Ulva* blooms. It was hypothesized that restored and natural marsh sediments would respond differently to acidification. For the restored marsh site, it was hypothesized that acidified conditions would enhance denitrification by fertilizing the

chemoautotrophic nitrifiers with CO_2, and therefore providing more NO_3^- for denitrifiers. For the natural marsh, it was postulated that acidification would not increase denitrification, but these sediments instead would demonstrate enhanced N-recycling due to higher organic C content and H_2S levels. It was also hypothesized that a cometabolism effect was likely to be evident in both sites because of seasonal *Ulva* blooms, but that decomposition would be higher in the natural site because greater C availability may sustain more microbial activity. To address these hypotheses, a continuous-flow, intact sediment core incubation was conducted using site water at ambient and acidified pH levels, and standardized tea litter bags (Tea Bag Index [TBI]) were employed, following Keuskamp et al. 2013, and adapted for use in salt marshes by Mueller et al. 2018. Seawater pH, dissolved oxygen, and quantified *Ulva* biomass were monitored at each marsh site.

METHODS

Site Overview

Jamaica Bay, New York, USA, is a heavily urbanized, 5260-ha embayment situated within the Hudson-Raritan Estuary system. It receives seawater input from the Atlantic Ocean via a narrow inlet, and experiences some of the highest levels of N inputs per unit area, largely from wastewater effluent, of any estuary worldwide (Howarth and Marino 2006; Hoellein and Zarnoch 2014). The average depth of the bay is approximately 5 m, but this average is heavily influenced by dredging activities that have significantly altered bathymetry from natural and historic contours (Hartig et al. 2002). The salt marsh complex within the bay has sustained marsh area loss within the last

century, with 15% estimated remaining. Some marsh islands have been restored to historic elevations within the few last decades, while some remain degraded due to low elevation and erosion (NYC Parks 2012). The Elders East marsh (40.635641, -73.845940) underwent restoration in 2006. Due to its higher elevation, it is now inundated an average of 6.4 $hrs^{-1}day^{-1}$. The marsh at Black Bank (40.614827, -73.83583) is a degraded site that has not been restored. With its lower elevation, it is inundated for an average of 8.95 $hrs^{-1}day^{-1}$ (Alldred et al. 2020). These two sites (Figure 1) were selected due to their contrasting restoration history and their proximity to each other, which results in similar environmental conditions.

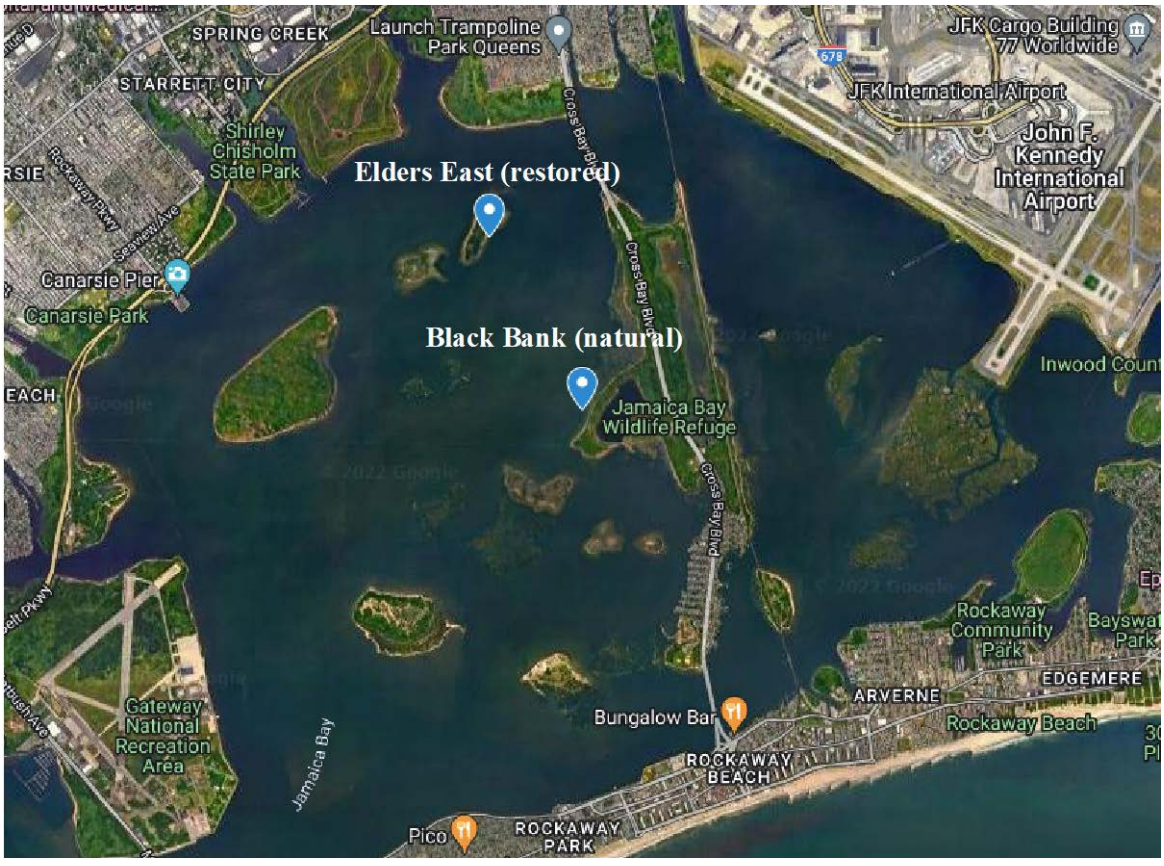

Figure 1: Map of the study sites within Jamaica Bay, New York, USA.

Ulva *Biomass Survey*

At each study site, 50m transects parallel to the water's edge, were established in three marsh zones: high-intertidal (adjacent to the marsh edge), low-intertidal (along the low-tide line), and mid-intertidal (intermediate to high and low zones). At Elders East, the width between high to low transects was 50 m, while at Black Bank the width was 30 m between high and low transects. Five 0.25 m^2 quadrats were randomly placed along each transect. All *Ulva* spp. was removed from each quadrat and transferred to sample bags for transport. *Ulva* samples were taken to the laboratory, where they were rinsed with tap water to remove sand and fouling organisms and blotted dry. Samples were then placed in a drying oven at 60 ºC to remove water. The dry mass was recorded after 48 h (Lamb 2018).

Teabag Study

The Tea Bag Index (TBI) uses a standardized litter of green and rooibos (red) teabags to calculate decomposition rates of labile and recalcitrant C respectively (Keuskamp et al. 2013) and has been adapted for use in salt marshes by Mueller et al. (2018). Lipton® green (EAN: 8722700055525; Lipton, Unilever, UK) and rooibos teabags (EAN: 8722700188438, Lipton, Unilever, UK) were weighed initially and organized into pairs in three different treatment types: green-only pair (G), rooibos-only pair (R), and a combined rooibos + green pair (C), comprising of a combination of one green and one rooibos teabag. Six of each treatment type per site (N = 18 pairs per site) were buried at depths of ~8 cm, at intervals of 2 m along the marsh edge (Mueller et al.

2018). Each pair was marked with a 0.3 m length of PVC pipe and a marker flag for ease of retrieval after the 90-day incubation period specified by Keuskamp et al. (2013).

Teabags were deployed on 15 July 2021 and retrieved on 8 October 2021, for a total of 95 days. Some replicates were lost during the incubation period: four replicate pairs out of six of each treatment were retrieved from Elders East, while five green-only, five rooibos-only, and three combined rooibos/green replicate pairs out of six were recovered from Black Bank. Each remaining pair was brought back to the lab where bags were rinsed with tap water to remove sediment and placed in a drying oven at 60ºC for 72 h. They were then weighed to determine dry mass. The dry mass lost over the 90-day incubation period was used to calculate the decomposition rate (*k*, a unitless value) and the inhibitory effect of the environment on decomposition known as the stabilization factor (*S*). The *k* and *S* parameters were calculated using the following formulas (Keuskamp et al. 2013; Mueller et al. 2018):

$$W_r(t) = a_r e^{-kt} + (1-a_r) \quad \text{(Eq. 1)}$$

$$S = 1 - a_g/H_g \quad \text{(Eq. 2)}$$

$$a_r = H_r(1 - S) \quad \text{(Eq. 3)}$$

In Eq. 1, $W_r(t)$ represents the remaining mass of rooibos tea after *t* incubation days; a_r is the labile portion of rooibos material while 1 - a_r is the recalcitrant portion. *S* is the stabilization factor; a_g is the fraction of green tea that is decomposable, while H is the hydrolysable fraction of the green tea (Eq. 2). Eq. 3 was used to determine the decomposable fraction of rooibos tea based on the hydrolysable fraction of red (H_r) and *S*. H_g and H_r values were given by Mueller et al. (2018) and have been used in calculations by Mozdzer et al. (2021).

Marley et al. (2019) suggested that mass loss/decomposition rate of organic matter may be an imperfect proxy for C consumption; therefore, elemental analysis, using a Perkin Elmer 2400 Series II CHN elemental analyzer, was performed on the remaining tea and undecomposed tea material that had also been dried at 60 ºC. %C for tea litter was converted to $mol^{-1}g$ for analyses.

Environmental Data Collection

HOBO dataloggers (Onset, Wareham, MA, USA) were installed at both the Elders East and Black Bank sites to collect pH, salinity, dissolved oxygen (DO), and light levels. Loggers were cable-tied to a cinderblock and deployed below the low tideline within an *Ulva* bed at each site for constant submersion. Salinity, DO, and light loggers were programmed to collect data every fifteen minutes over a 24-hour period and were deployed from August 2021 through October 2021. pH loggers were configured to record readings every minute, with readings taken 24 hours daily from August 2021 through September 2021, to capture diel fluctuations during the peak of the *Ulva* growing season (Wallace and Gobler 2015). Readings from the HOBO loggers were taken using the NBS scale (pH_{NBS}) and corrected to total pH scale (pH_T) by subtracting the average offset (~0.2) between NBS and total scale readings ($pH_T < pH_{NBS}$). Average offset was determined by the mean difference between pH_{NBS} meter readings and pH_T values that had been converted using TRIS/AMP calibration calculations (Lowell et al. 2021). Data was offloaded approximately bi-weekly and loggers recalibrated as needed during the deployment period. Daily pH and DO ranges were calculated by subtracting the minimum reading value for each 24-hour period from the maximum reading value.

Additionally, seasonal pH and DO ranges were computed by calculating the mean of assembled daily ranges.

Continuous-Flow Sediment Core Incubation

On 16 September 2021, intact sediment cores (N = 16) were collected from the Elders East and Black Bank marshes, using acrylic cylinders (30 cm in length, 7.6 cm diameter) (Gardner et al. 2006). Eight cores were collected from each site at the marsh edge at least 2 m apart from each other and were selected to exclude *Spartina* stems. Cores were taken within a distance of ~0.25 m of where teabag replicates had been buried, so that conditions of decomposition and nutrient cycling were comparable; care was taken to avoid disturbing the sediment immediately surrounding teabag burial sites. Sediment depth in the cores was between 12-15 cm. Cores were sealed at both ends with rubber caps and transported to the laboratory in a dark cooler (~2 hours). Any *Ulva* on the sediment surface or macrofauna were removed from the cores.

Site water was collected in five 20 L carboys from Pumpkin Patch Channel, which is a navigable channel that connects the two study sites and transported back to the laboratory for use in continuous-flow core incubations. An Accumet Basic AB15 Plus pH meter (Fisher Scientific, Waltham, MA, USA) fitted with a TRIS-compatible Accumet electrode was calibrated to total pH scale (pH_T) using TRIS and AMP buffer calibration curves (Lowell et al. 2021) and used to determine pH_T of site water treatments. Half of the site water was kept at ambient pH (pH_T ~7.86). The other half was acidified by bubbling 7 ml min^{-1} of pure CO_2 mixed with air by a gas proportioner to maintain an average pH_T of 7.23. This was a slightly higher concentration of CO_2 than used by

Lowell et al. (2021), who used 5 ml min^{-1}; pH_T did not drop sufficiently at that concentration in this experiment. The mean difference of ~0.6 pH units between treatments was determined to simulate average diel fluctuations in pH recorded by the HOBO dataloggers around the time of sampling, and within the range of acidification events described by Wallace et al. (2014).

In the laboratory, half of the cores from each site (n=4) were treated for acidified conditions and the other half were selected for ambient conditions. Each core was filled to a volume of ~230 ml of either ambient or acidified site water depending on the treatment. All cores were sealed at the bottom with a rubber cap and at the top with a plunger fitted with an O-ring to maintain air-tightness. Each plunger contained an inlet and outlet hole plumbed with polyetherketone (PEEK) tubing (Zeus Inc., Branchburg, NJ, USA). Cores were incubated in a water bath kept at 23 ºC and under dark conditions to prevent photosynthesis.

Aerated ambient site water and mixed CO_2/air acidified site water were pumped through the intact cores at a rate of 1.1 ml min^{-1}, with a turnover time of 4.2 hours, for a 24-hour incubation period. At the end of the incubation, water samples were taken directly from each inflow header tank as well as from each core outflow and filtered into triplicate 20 ml scintillation vials, then frozen until they were analyzed for nutrient content (NH_4^+, nitrite [NO_2^-], NO_x [NO_2^- + NO_3^-], and soluble reactive phosphorus [SRP]). Inflow and outflow samples were also collected for gas analysis by filling three replicates per core of 12 ml borosilicate exetainer vials (Labco Ltd., Lampeter, United Kingdom). Each exetainer was filled by placing the end of the outflow tube at the bottom of each vial and allowed to overflow for several volumes. These were then preserved

with 200 µl of 50% zinc chloride (McCarthy et al. 2007). Exetainer vials were then carefully capped to minimize introduction of air bubbles and stored submerged in water at 4 ºC until gas analysis was performed. The pH for all treatments was monitored throughout the trial period.

Nutrient and Gas Analysis

Dissolved inorganic nutrients were measured from core-incubation water samples on an AQ300 Autoanalyzer (Seal Analytical, Inc., Mequon, WI). The phenol hypochlorite method was used to measure NH_4^+ (Solorzano 1969), and the antimonyl tartrate method was used for SRP measurements (Murphy and Riley 1962). NO_x^- was measured with cadmium reduction while NO_2^- was measured without cadmium reduction (APHA 1998).

Dissolved gas measurements ($^{28}N_2$, $^{32}O_2$, and ^{40}Ar) were taken using a membrane inlet mass spectrometer (MIMS; Bay Instruments, Easton, MD; Kana et al. 1994). Artificial seawater (25 PSU) bath was used as a standard. The seawater bath was kept at a constant temperature (23 ºC; Circulating Bath, VWR International, Radnor, PA) and equilibrated to atmospheric gases by stirring (Lab Egg RW11 Basic, IKA Works, Inc., Wilmington, NC).

Sediment Characteristics

After core incubations were completed, three 15 ml replicates of sediment were collected from the top ~2.5 cm of each core and refrigerated at 4 ºC overnight for processing for organic matter (OM), %C, %N, and porosity. For OM content, 5 ml from

each core were dried in a drying oven at 70 ºC for two days, then ashed in a muffle furnace at 500 ºC for four hours (Benfield 2006). For %C and % N content, dried sediment samples were treated twice with 25% HCl (Nieuwenhuize et al. 1994) and then re-dried. These were then measured on a Perkin Elmer 2400 Series II CHN Analyzer (Perkin Life and Analytical Sciences, Shelton, CT). %C and %N were converted to μmol C and μmol N for statistical analysis. Averages of C and N were calculated for each core.

Statistical Analysis

Ulva biomass was compared using mixed-effect models. Biomass among marsh zones was assessed with transect used a random effect to account for within-transect heterogeneity and pseudoreplication (Zuur 2009; Bates 2010). *Ulva* was also compared between sites using transects and quadrats as random factors.

Mixed-effects models were also used to compare mass loss of combined rooibos-green tea treatments to rooibos-only treatments, to test for a cometabolism effect between sites and treatments. Decomposition rates (*k*), tea mass loss, and C loss were calculated for each tea bag pair, and linear mixed models were conducted to assess differences in *k*, mass loss, and C loss across sites and treatments, using tea bag pair number as a random effect to account for pseudoreplication. Proportions of C loss and mass loss were arcsine-transformed for use in modeling.

Nutrient and dissolved gas flux replicates were averaged for each core. Pearson's product-moment correlational analyses between mean fluxes were performed to determine relationships among nutrient and gas fluxes. Significantly correlated relationships were further analyzed using mixed models with sites as random effects to

address within-site pseudoreplication. Core means were calculated for all sediment characteristics and then analyzed using mixed effects models with sites as a random effect.

For all regression models, residuals were visually checked for homogeneity and normality. *P*-values of ≤ 0.05 were considered to be statistically significant, and in mixed-effects models, *p*-values were generated using analysis of Type III sums of squares models (Fox and Weisberg 2011). Significant differences among treatments were identified using Tukey post-hoc methods (Zarnoch et al. 2017; Zhu et al. 2019).

All statistical analyses except for pH/DO range calculations were conducted in RStudio v. 1.1.423 (R Core Team 2020). All figures were produced using the R package 'ggplot' (Wickham 2016). Models were conducted using the 'lme4' package (Bates et al. 2015), and Tukey post-hoc tests were done using the package 'multcomp' (Hothorn et al. 2008). Environmental data (pH/DO) ranges and averages were calculated using Microsoft Excel v. 16.33 (Microsoft Corporation 2020).

RESULTS

Ulva *Biomass Survey*

Ulva spp. biomass differed significantly between marsh zones ($p = 0.017$; $\chi^2 = 8.11$) as well as interactively between sites/marsh zones ($p = 0.034$; $\chi^2 = 6.79$) (Figure 2). Most of the total biomass (62.7%) from both sites was concentrated in the low-intertidal zone. At Black Bank, 49.3% of the biomass was found in the mid-intertidal zone, while 0% was found in mid-intertidal quadrats at Elders East. Both Black Bank and

Elders East had less *Ulva* accumulation along the high-intertidal marsh edge than the low-intertidal zone, with 5.7% and 6.9% respectively.

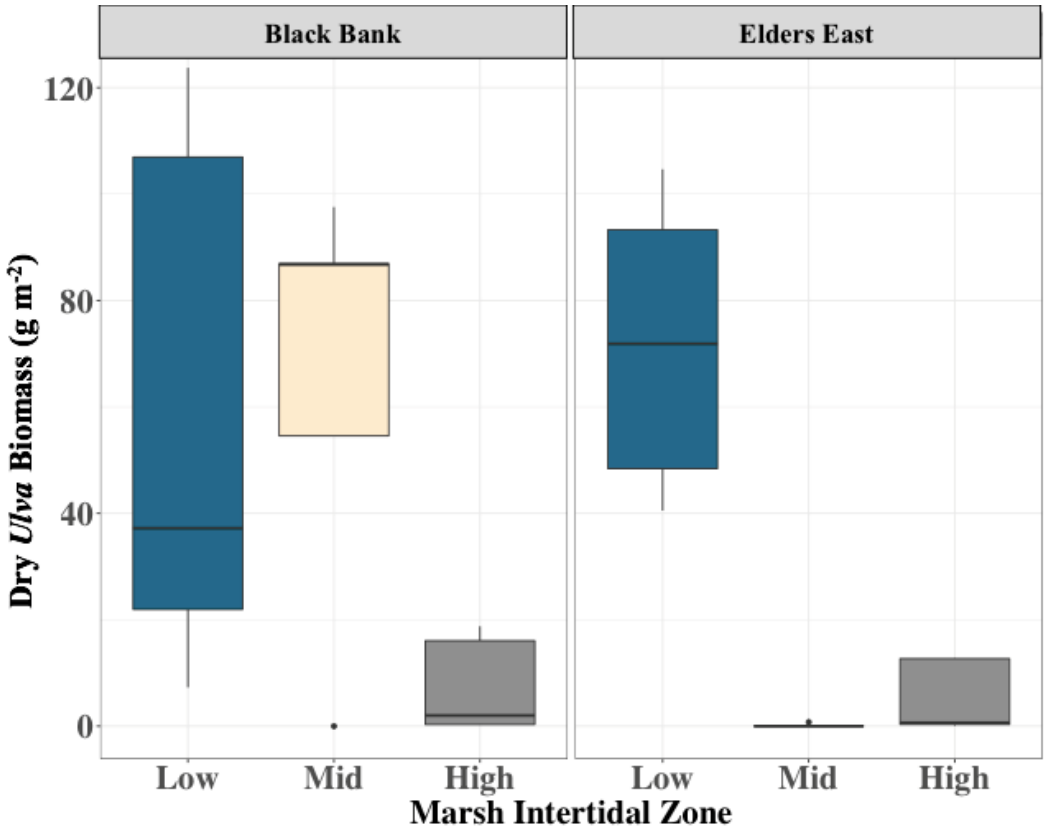

Figure 2: ***Ulva*** **Biomass in Black Bank and Elders East. Dry** ***Ulva*** **biomass collected in the low-, mid-, and high-intertidal marsh zones. Overall biomass did not significantly differ between sites or zones, but distribution of macroalgae did differ between Black Bank and Elders East.**

Tea Bag Study

Green teabags at Elders East lost an average of 78.8% (SEM = 0.48) of their mass, and 76.1% (SEM = 1.71) of their mass at Black Bank (Figure 4A). Rooibos teabags lost 33.8% (SEM = 0.84) at Elders East, and 31.6% (SEM = 1.51) at Black Bank (Figure 4A). Green teabags from Elders East lost an average of 0.49% of their C (SEM = 0.070),

and green teabags at Black Bank lost an average of 9.5% of C (SEM = 1.73) from. Rooibos teabags in the Elders East marsh lost a mean of 1.9% (SEM = 1.08) of their C, and rooibos teabags in the Black Bank marsh lost a mean of 5.8% (SEM = 0.76) of their organic C (Figure 4B). Rooibos-only teabags at Black Bank had a significantly higher *k* than rooibos-combined teabags ($p = 0.055$; $\chi^2 = 2.97$; Figure 3). There was no significant difference in *k* between rooibos-combined and rooibos-only teabags at Elders East. Furthermore, at both sites, % mass loss (Figure 4A) and % C loss (Figure 4B) did not differ between rooibos-only and combined-rooibos treatments.

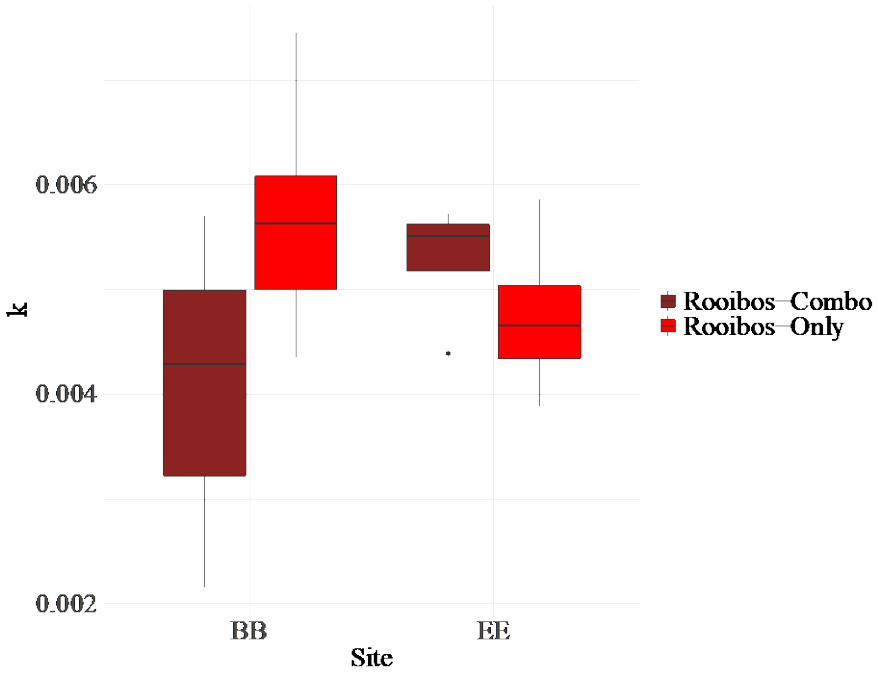

Figure 3: **Decomposition rates (k) between Black Bank (BB) and Elders East (EE). Rooibos-only teabags at Black Bank had a significantly higher decomposition rate than rooibos bags in combined treatments. There was no significant difference between treatments at Elders East. Green teabags are not shown here because *k* calculations require mass loss of rooibos.**

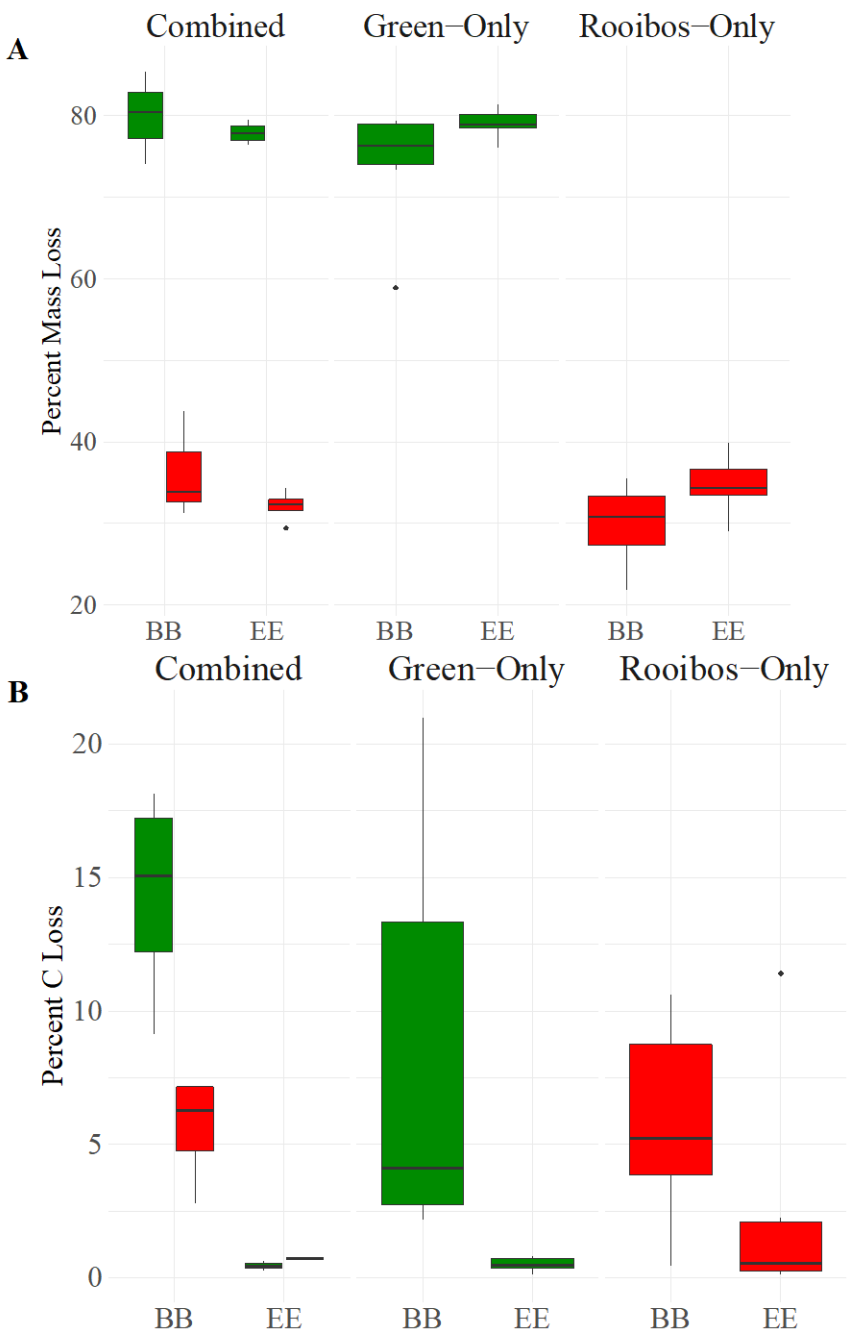

Figure 4A,B: Percent mass and C loss in teabags across sites. Green teabags in both combined and green-only treatments lost a higher proportion of mass and C content than rooibos bags. %Mass loss and %C loss did not, however, differ significantly between combined-rooibos and rooibos-only bags at either site, suggesting no cometabolism effect.

Environmental Data

Average diel pH_T fluctuations were similar between Black Bank and Elders East throughout the month of August, with a mean range of 1.28 pH units at Black Bank and 1.32 pH units at Elders East. From 2 August through 1 September, diel fluctuations had up to a total range up to 2.31 pH units at Black Bank and 2.27 pH units at Elders East. Each day, pH_T was highest in the afternoon (~3:00-6:00pm) and lowest just before dawn (~3:00-6:00am). Fluctuations began to lessen in amplitude after 26 August (an average diel range of 0.67 at Black Bank and 0.65 at Elders East from 27 August through 1 September, the last day of logger deployment). From 27 August through 1 September, pH_T at Black Bank did not rise above 7.91, and 8.16 at Elders East (Figure 5).

The pH_T values were positively correlated with DO readings in both sites ($p < 0.001$; Figure 6). DO was also significantly correlated with water temperature ($p < 0.001$). From 2 August to 27 August, DO reached supersaturated levels (>100% saturation) in the afternoon, some nights dropping to complete anoxia (0% saturation) just before dawn, with a diel range of 30.55 $mg^{-1}L$. DO levels had a lower diel range from 28 August through 18 September (20.68 $mg^{-1}L$) than earlier in the month (Figure 7).

Recordings of pH and DO also followed a biweekly pattern, where peaks decreased in amplitude relative to other weeks. One of these occurred between 14-17 August (a range of 0.68 pH units/8.55 mg L^{-1} DO) compared with the week prior, where the range was 1.72 pH units/15.82 mg L^{-1} DO. These periods of decreased pH and DO range also occurred between 29 August and 1 September (0.9 pH units/10.85 mg L^{-1} DO), compared with the previous week (1.86 pH units/21.43 mg L^{-1} DO). DO continued to show this pattern after pH loggers stopped recording data, with similar

decreases in peak amplitude around 15 September and 30 September, which corresponded with a half-moon/ neap tide event (NOAA 2021; Figure 7).

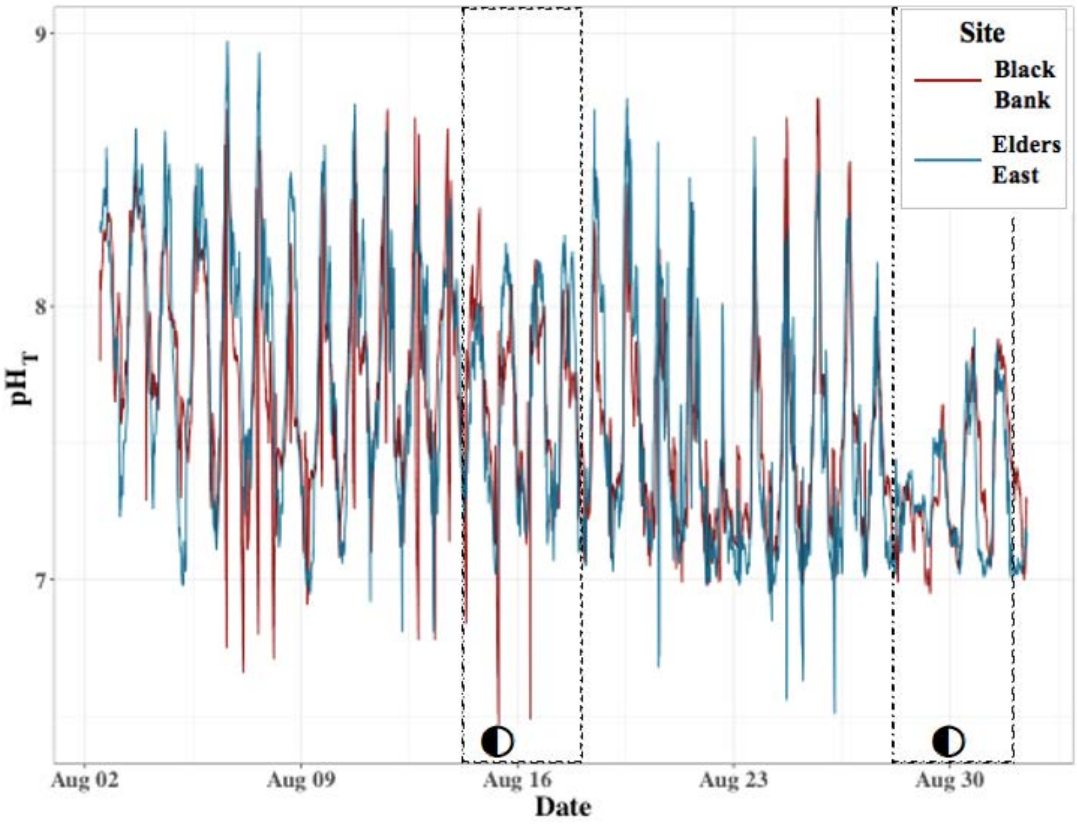

Figure 5: **Total pH (pH$_T$) during datalogger deployment. Seawater pH in both study sites showed diel fluctuations, which lessened in amplitude towards the end of the deployment period. Periods of lower pH fluctuation (~14-17 Aug) and (~29 Aug-1 Sep) corresponded with neap tides, indicated by dashed lines. The half-moon occurred on 15 and 30 August, indicated by half-filled circles (NOAA 2021).**

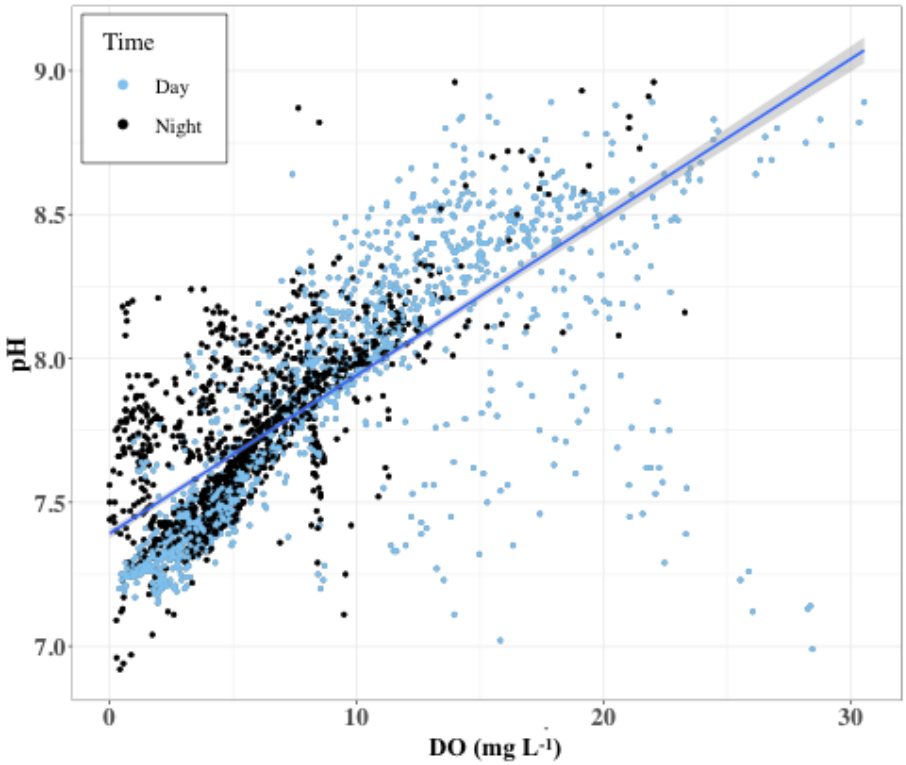

Figure 6: **Daytime and nighttime dissolved oxygen (DO) levels compared with pH. DO significantly correlated with seawater pH (this figure shows results from Black Bank only, as some DO data for Elders East was not available). Shading indicates 95% confidence intervals.**

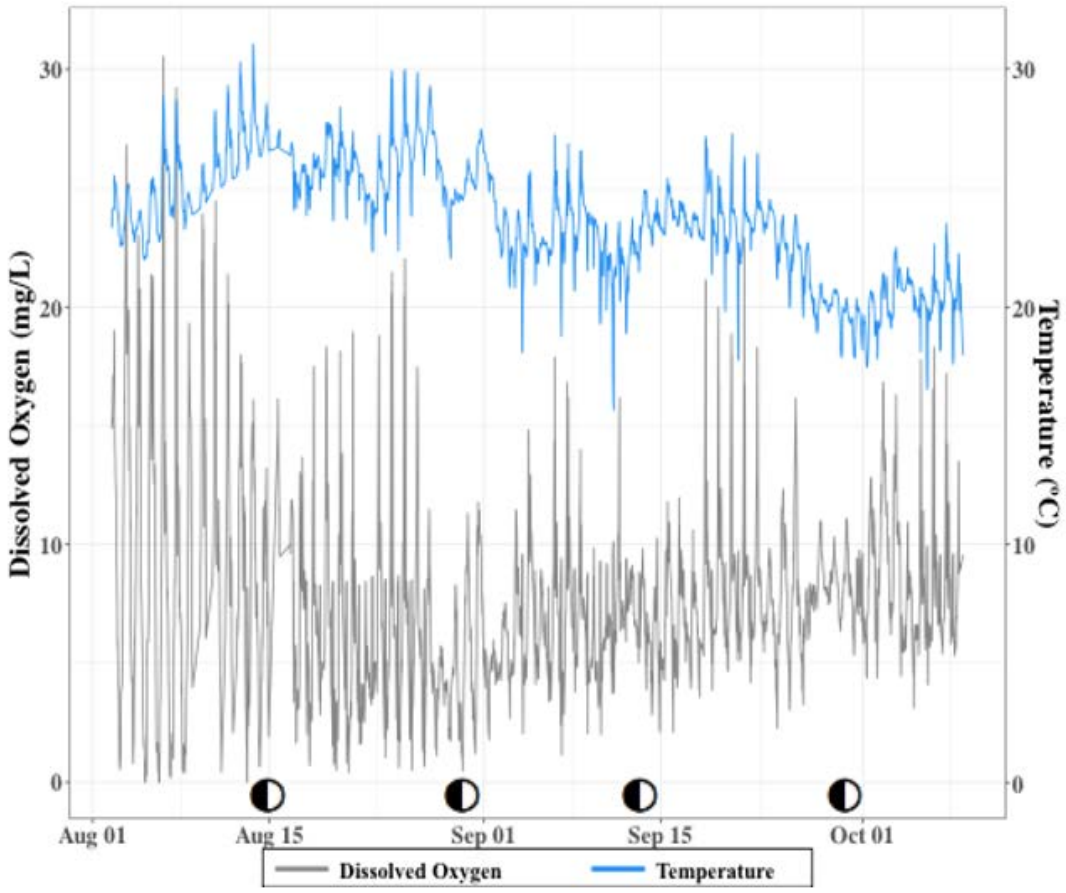

Figure 7: **Dissolved oxygen (DO) and seawater temperature. This figure encompasses the deployment period for Black Bank dataloggers, as some data for Elders East was unavailable. Half-filled circles indicate the half-moon, when neap tides occurred (15 Aug., 30 Aug., 13 Sept., and 29 Sept. (NOAA 2021).**

Nutrient and Gas Analysis

Dissolved inorganic nitrogen (DIN) fluxes were not significantly different between acidified and ambient treatments at either site (Figure 8). NO_x^- uptake and NH_4^+ efflux did not differ between ambient/acidified treatments in either Black Bank or Elders East, and there were no significant interactions between site/treatment and N flux.

Similarly, N_2 efflux (Figure 8) and sediment oxygen demand (SOD; Figure 9) did not significantly differ between ambient and acidified cores. The only nutrient flux that

differed between ambient and acidified treatments was SRP, at Black Bank only (p = 0.021, R^2 = 0.55, $F_{1,6}$ = 9.70). Ambient-pH cores had a negative flux of SRP, indicating net uptake, while acidified cores from Black Bank had positive fluxes, suggesting release of P (Figure 8).

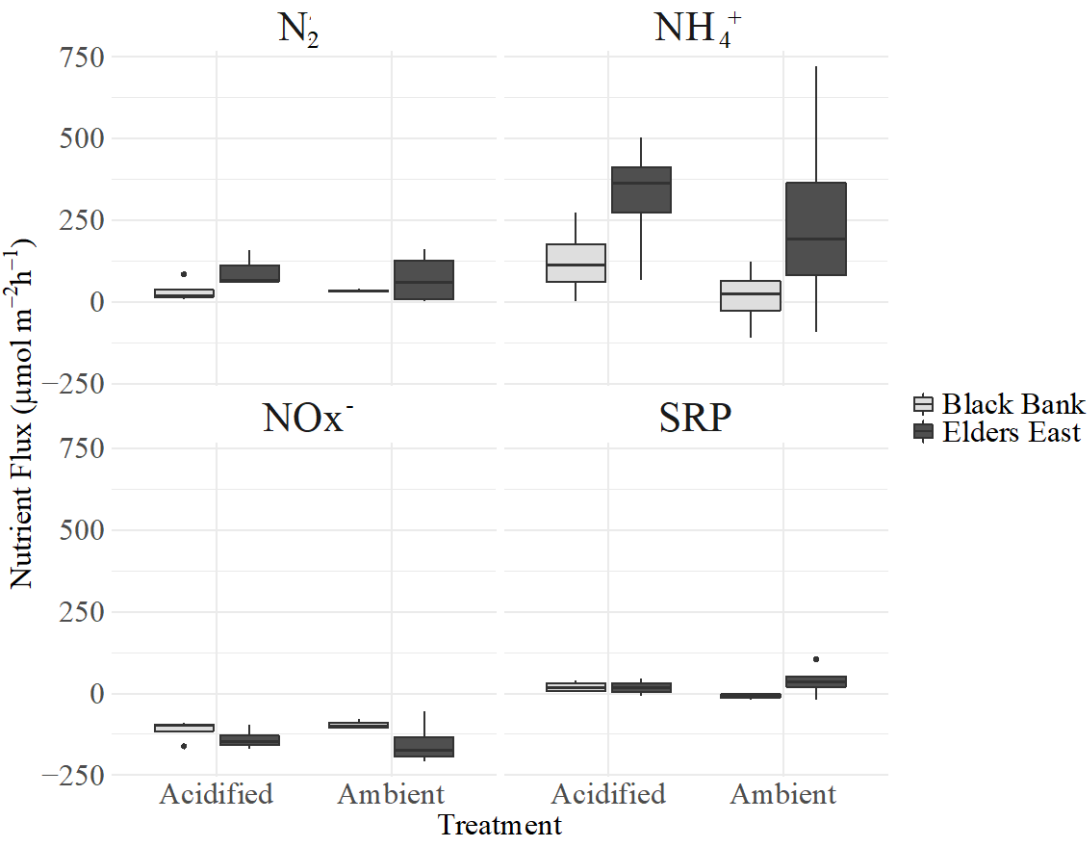

Figure 8: **Nutrient and gas fluxes from sediment cores. N fluxes did not significantly differ between ambient/acidified core treatments in either site. A negative flux indicates uptake, while a positive flux indicates efflux.**

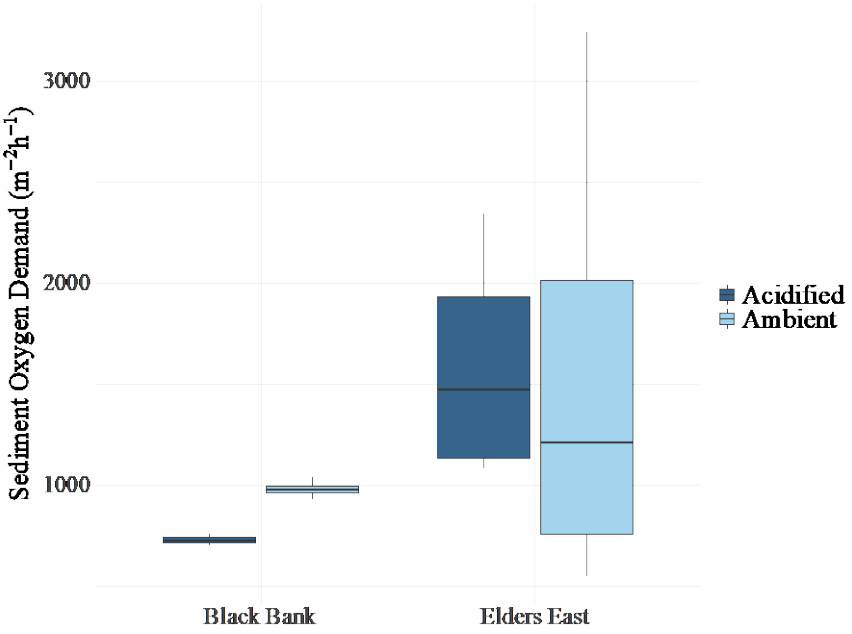

Figure 9: **Sediment oxygen demand from cores. Elders East sediments in both ambient and acidified treatments had a higher oxygen demand than those at Black Bank, but there was not a significant difference between pH treatments at either site.**

There were, however, differences in DIN fluxes between the two marsh sites. NO_x^- (NO_2^- and NO_3^-) uptake (indicated by negative fluxes) was significantly higher at Elders East ($p = 0.007$; $\chi^2_2 = 7.144$). NH_4^+ efflux (indicated by positive flux values) was also significantly higher at Elders East than Black Bank ($p = 0.016$, $\chi^2_2 = 5.86$; Figure 8). NO_x^- uptake, as well as NO_3^- and NO_2^- alone, significantly correlated with NH_4^+ efflux ($p < 0.001$ for all; $\chi^2_2 = 23.60$; Figure 10A). The concentration of NO_x^- in both inflow header tanks averaged 33.6 µM (SEM = 0.006) and concentration of NH_4^+ averaged 31.4 µM (SEM = 0.02).

Dissolved gas fluxes and their relationships with DIN fluxes also differed between sites but not between pH treatments. Sediment oxygen demand (SOD) was significantly higher at Elders East than Black Bank ($p = 0.039$; $\chi^2_2 = 4.28$; Figure 9), as was N_2 efflux ($p = 0.018$, $\chi^2_2 = 5.55$; Figure 8). Net N_2 fluxes correlated positively with

NO_x^- uptake at both sites overall ($p < 0.001$; $\chi^2_2 = 16.82$), but separated by site, only Black Bank had a relationship with NO_3^- ($p_B = 0.046$, compared with $p_E = 0.0808$; Figure 10B). SOD and N_2 efflux were positively correlated at both sites ($p = 0.001$ for both; Figure 10C). SRP was positively correlated with DIN fluxes, N_2 flux, and SOD ($p \leq 0.001$ for each; data not shown).

Sediment Characteristics

Sediments from Black Bank contained significantly higher C and N than samples from Elders East ($p_C < 0.001$, $R^2_C = 0.371$, $F_{1,46} = 28.69$; $p_N < 0.001$, $R^2_N = 0.337$, $F_{1,46} = 24.83$); Black Bank sediments contained higher organic C than Elders East ($p = 0.032$; $R^2 = 0.255$; $F_{1,13} = 5.78$) and had a greater proportion of water to sediment, i.e., were more porous ($p = 0.009$; $R^2 = 0.37$; $F_{1,13} = 9.303$). Black Bank sediments also contained higher organic matter (OM) than Elders East sediments ($p = 0.011$; $R^2 = 0.36l$; $F_{1,13} = 8.84$). Elders East samples were more dense than Black Bank samples ($p = 0.057$; $R^2 = 0.194$; $F_{1,13} = 4.377l$). All site means and standard errors are presented in Table 1.

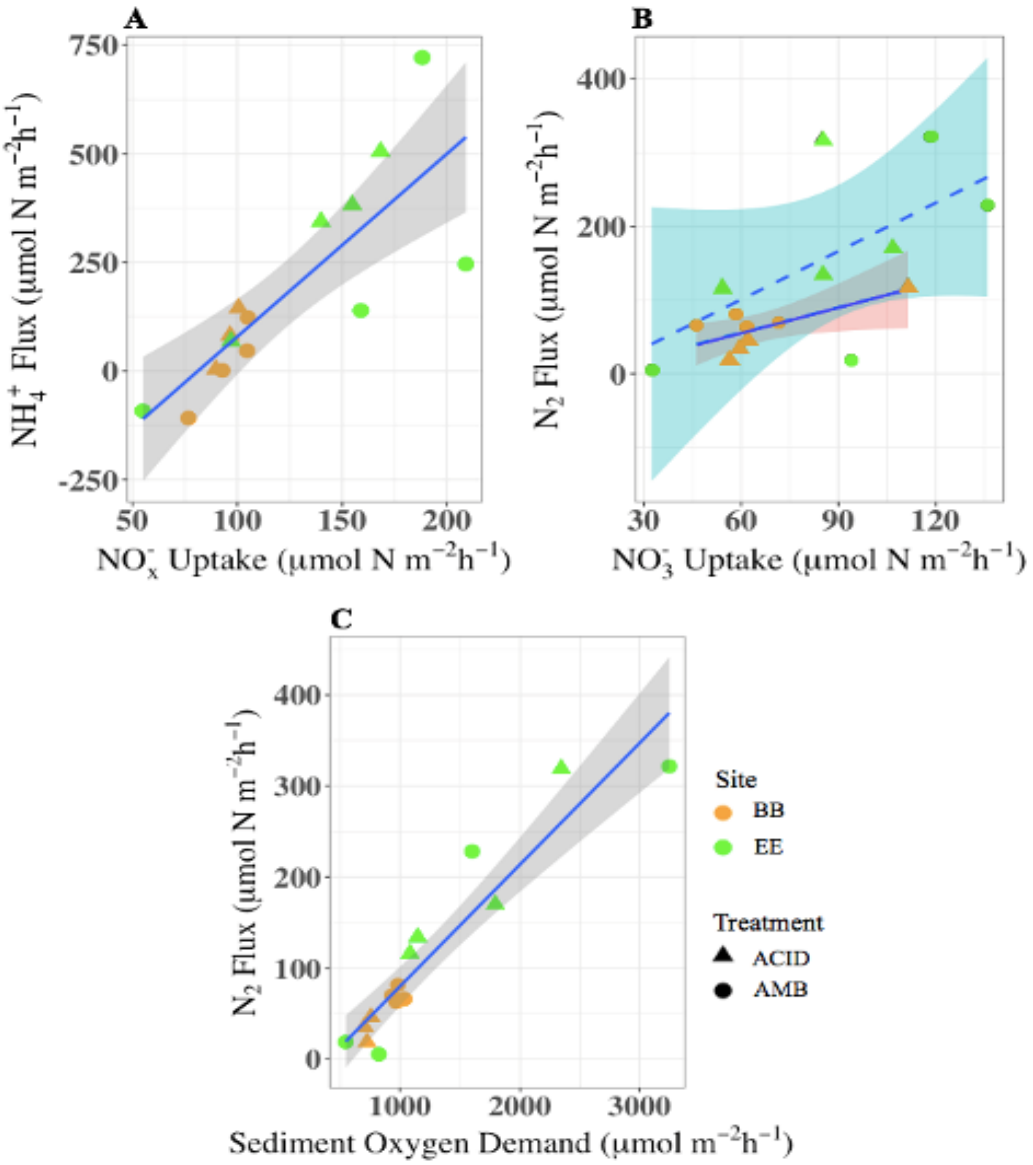

Figure 10A: **Nutrient and dissolved gas relationships. NO_x^- uptake correlated with NH_4^+ efflux at both sites (both higher at Elders East [EE] than Black Bank [BB]), but there were no differences between ambient (AMB)/acidified (ACID) treatments.**

Figure 10B: **Nitrate uptake had a significant relationship with N_2 production at Black Bank (solid line), which can be indicative of direct denitrification. The relationship between these two N species was less clear at Elders East (dashed line), likely the result of multiple outliers. Light-blue and pink shading surrounding trendlines indicates 95% confidence intervals.**

Figure 10C: **Sediment oxygen demand was positively related to N_2 efflux at both sites, irrespective of pH treatment. For 9A and 9C, gray shading indicates 95% confidence intervals.**

Table 1: **Sediment characteristics. %C, %N and organic C, and organic matter content were significantly higher in Black Bank sediments than Elders East cores. Elders East sediments were more dense and less porous than at Black Bank.**

Site		%C g^{-1}	%N g^{-1}	µmol C g^{-1}	Bulk Density (g cm^{-3})	Porosity (Proportion Water/ Sediment)	%Organic Matter (OM)
Black Bank	Mean	2.76 (±0.49)	0.21 (±0.04)	465.05	1.56 (±0.26)	0.44 (±0.07)	6.15 (±1.76)
Elders East	Mean	0.14 (±0.01)	0.02 (±0.002)	13.82	2.25 (±0.18)	0.21 (±0.04)	0.54 (±0.028)

DISCUSSION

This study explored how acidification and cometabolism may alter ecosystem processes in natural and restored salt marshes in Jamaica Bay. It had been predicted that acidification would amplify denitrification response in cores from the restored marsh and promote N recycling in the natural marsh. A cometabolism effect was expected to be visible in both sites in the tea bag study, and that this effect would be particularly pronounced in the natural marsh; however, it was discovered that neither acidification nor cometabolism appear to significantly impact marsh N-cycling or decomposition respectively. The former may be a result of marsh microbial communities becoming acclimatized to pH shifts, or that nitrifiers may not increase their activity due to increased CO_2, as initially hypothesized. Cometabolism of recalcitrant litter material in the presence of labile litter was not observed at either site, likely a result of unstable

early-stage decomposition dynamics. Instead, it is likely that other processes and environmental factors may have played a more significant role in biogeochemical cycling and decomposition at the time of study, such as hydrogen sulfide release or NH_4^+ mineralization from decomposing *Ulva*, the tidal/hydrological conditions at the time of sampling, and length of deployment time for tea litterbags.

Ulva *Biomass Survey and Teabag Study*

Annual *Ulva* growth cycles were monitored in previous studies, and these seem to follow a similar temporal pattern to low DO/low pH conditions demonstrated by Wallace et al. (2014). The peak of *Ulva* growth in Jamaica Bay has been described as occurring in July/August (~146 g dry weight m^{-2}), with subsequent sharp declines in *Ulva* biomass that reach their lowest point in September (~38 g dry weight m^{-2}; Lamb 2018). The mean maximum biomass between the two sites in this study was higher, with 523.2 g dry weight m^{-2}, and were collected on 2 August 2021. Other studies of eutrophic systems in Europe showed similar temporal growth cycles, with the lowest or zero *Ulva* mass occurring between August and September at similar latitudes (Coffaro and Sfriso 1997; Malta and Verschuure 1997; Malta et al. 2002).

While mean *Ulva* accumulation overall did not differ significantly between Elders East and Black Bank, distribution of algae between the two sites was not entirely equivalent. Black Bank contained *Ulva* in all three of its transect zones (low-, mid-, and high-intertidal zones), while the Elders East mid-intertidal transect contained none. This may have been due to patterns of inundation because *Ulva* and other macroalgae are more likely to accumulate in areas with lower elevation and higher tidal flooding

(Valiela et al. 1997). As Black Bank is flooded on average of 8.95 hours per day compared with 6.4 hours per day at Elders East (Alldred et al. 2020), these distribution patterns seem appropriate. It does not appear to be unusual that *Ulva* was found in the high-intertidal zones in this survey; in fact, high-intertidal abundances found here were significantly lower than those described in Rhode Island marshes described by Newton and Thornber (2012), where ~80% of the biomass occurred within the first two meters of the *Spartina alterniflora* marsh edge.

Despite the possibility for *Ulva* to have accumulated along the marsh edge for the duration of the growing season, a cometabolism effect did not appear to occur at either site. The initial prediction for thus study was that rooibos teabags in combined treatments would show significantly higher decomposition rates (*k*) and mass loss than teabags in rooibos-only treatments, indicating a cometabolism effect. It was anticipated that this effect would be particularly strong at Black Bank. However, the opposite was observed: that the rooibos-only treatment at Black Bank had a significantly higher *k* than rooibos bags from combined treatments. This may have been the result of a combination of environmental and temporal factors. First, tea bag transects contained a high degree of habitat heterogeneity, particularly at Black Bank. Because the marsh is unevenly fragmented (Campbell et al. 2017), the transect contained significant heterogeneity in vegetation and sediment conditions. In contrast, the study that demonstrated cometabolism effects in seagrasses conducted a litterbag experiment in a mesocosm, rather than *in situ*, so the researchers were able to control for inundation, aeration, and temperature (Liu et al. 2020). Thus, a 95-day deployment period may not have been a sufficient amount of time for a cometabolism effect to become visible.

While ~90 days is recommended by Keuskamp et al. (2013) for incubation across habitat types (including wetlands), Mozdzer et al. (2021) suggested that this length of time in salt marshes only captures the earliest stages of decomposition *in situ*. Similarly, Marley et al. (2019) recommended that teabags be deployed in marshes for at least a year, since decomposition dynamics within the first three months exhibit a high degree of instability in the field.

Despite the factors described above, rates of decomposition from this study fit in the lower end of the range for salt marshes across the Northeastern United States. The *k* values calculated in this study were intermediate to those calculated for marshes in Massachusetts and Maine (Mueller et al. 2018). Mean *k* values from this study were in range of, and sometimes equivalent to, *k* values found by Mozdzer et al. (2021), who deployed their teabags within 2m of the high-marsh zones of Massachusetts marshes. Decomposition rates of 0.005-0.006 like those found in this study have also been described in other aquatic habitats such as lake sediments and mangrove swamps (Keuskamp et al. 2013; Seelen et al. 2019).

pH and DO Fluctuations Reflect Temporal and Tidal Patterns

During the study period, pH cycles fluctuated over 24-hour periods as well as throughout the month-long datalogger deployment. Near the end of the deployment period, readings appeared to transition from 24-hour diel pH cycles with differences of >2 pH units in early-to-mid August, to diel ranges of ~1 pH unit. In the core study, the pH_T of the inflow water (7.86) in the ambient treatment was consistent with daytime pH levels recorded at the end of August, while the acidified treatment (pH_T = 7.23) was

consistent with nighttime values during the same period. Total pH and DO correlated strongly ($p < 0.001$; Fig 6), as has been described in prior studies in Jamaica Bay, as well as in Long Island Sound, and Narragansett Bay (Wallace et al. 2014). Prior studies in Jamaica Bay have described conditions of hypoxia and low pH in the late summer with pH remaining relatively consistent at an average of 7.6 throughout September (Wallace et al. 2014).

Dataloggers also appeared to detect patterns in biweekly tidal cycles, and, to a lesser extent, diel tidal cycles. Biweekly periods were observed during which pH and DO ranges were lower than other biweekly ranges. These appeared to correspond with neap tides (NOAA 2021), which tend to have lower flushing rates than spring tides (Shaha et al. 2010). Spring tidal elevation peaks have been described to correspond with peaks in O_2 production (Kitheka et al. 1996). More extreme pH/DO range fluctuation during a spring tide may be due to an increase in macroalgal delivery into the marsh as a result of greater tidal input. Transport of macroalgal biomass into an estuary during a spring tide has been described to be 2 to 3 times higher than during a neap tide (Whitfield 1988). Spring tides also may introduce higher nutrient influxes than neap tides, fueling greater algal productivity (Webb and D'Elia 1980). Daily peaks in O_2 production and pH values in this study corresponded with daytime high tides (NOAA 2021), with ebb tides in the late afternoon and evening showing a steep decline in O_2, a pattern also observed by Gruber et al. (2017). Daytime low tides also had relatively high O_2 production despite low water levels; this is likely because diel patterns of algal productivity in estuaries tend to be primarily driven by photoperiod length rather than vertical stratification (Haro et al. 2019).

Acidification Had No Effect on Sediment N Cycling Processes

It was initially hypothesized that acidification would increase denitrification at the restored site due to CO_2 fertilization for autotrophic nitrifiers which could promote coupled nitrification-denitrification. In contrast, it was predicted that Black Bank, the natural, degrading marsh, would not be impacted by acidification, have reduced denitrification, and greater N recycling. This would be due to higher organic C stocks, anoxic sediments, and high hydrogen sulfide concentrations (Alldred et al. 2020) that could inhibit nitrification, and thus coupled nitrification-denitrification, as well as promote dissimilatory nitrate reduction to ammonium (DNRA). Although higher rates of denitrification were seen at Elders East, the acidification treatment did not enhance denitrification. As predicted, there was no effect of acidification at Black Bank. The lack of response to acidification at Elders East may be due to the microbial community being conditioned to diel fluxes of dissolved oxygen and low pH in the weeks preceding sediment core collection as indicated by the monitoring data (Figures 5 and 7).

The impact of low pH in eutrophic estuarine systems remains unclear. Previous research has demonstrated that low pH can have a negative effect on nitrification in open-ocean systems (Beman et al. 2011; Hutchins and Fu 2017) but has also been found to increase nitrification in estuarine systems (Fulweiler et al. 2011). However, other biogeochemical processes are co-occurring in these systems which can confound the effect of pH alone. In the core incubations the inflow water in the acidified treatments had low pH and high oxygen concentrations (i.e., saturated) due to aeration. Although these conditions differ from a coastal acidification event, they allowed us to

explore the single effect of low pH. The microbial communities in the sediment cores, however, were exposed to weeks of diel changes in oxygen and pH prior to core collection and the assemblage may have changed to a community adapted to these conditions (Kitidis et al. 2011). For example, ammonia-oxidizing archaea (AOA) have been observed to dominate over ammonia-oxidizing bacteria (AOB) at lower pH (Yao et al. 2011), but community shifts between these types of organisms may not necessarily result in a net change in nitrification rate (Bernhard et al. 2010). Gazeau et al. (2014) reported no changes to denitrification rates in acidified Arctic sediments and proposed that nitrification did not change due to the acidified conditions. It is likely that certain groups of nitrifying bacteria are responsive to acidification and the abundance of these may be related to environmental conditions. In Jamaica Bay, nitrifier activity remains relatively consistent throughout the course of a year (Lindemann et al. 2016; Hoellein and Zarnoch 2014). This may suggest that community composition may shift as a result of pH without changes to net nitrification, such as suggested by Bernhard et al. (2010), or that the communities found there are already composed of species that are more pH-resistant. Long-term studies are needed to identify how seasonal changes in pH may influence sediment N cycling in coastal ecosystems.

Site Differences

It had been hypothesized that the restored and natural sites would have differences in the measured gas and nutrient fluxes due to varying sediment carbon and oxygen conditions at each site (Alldred et al. 2020). It was predicted that the reduced sediment conditions at Black Bank would limit coupled-nitrification denitrification;

however, a positive relationship was found between sediment oxygen demand and N_2 flux among measurements from both sites (Figure 10C). This relationship is often considered an indicator of coupled nitrification-denitrification (Piehler and Smyth 2011; Seitzinger et al. 2006). Thus, it is likely that some coupled nitrification-denitrification was happening at both sites. Indeed, a positive relationship was also found between NO_3^- uptake and sediment oxygen demand at both sites suggesting coupled nitrification-denitrification (Vieillard and Fulweiler 2012). The magnitude of the O_2 and N_2 fluxes, however, were different between sites, which could suggest other important drivers of denitrification. Both coupled and direct denitrification have been observed to occur together in salt marshes in the northeastern United States (Hamersley and Howes 2005; Koop-Jakobsen and Giblin 2010). Direct denitrification is more common in ecosystems where water column nitrate is high, as was the case in this study (Seitzinger et al. 2006). Black Bank sediments had a significant positive correlation between NO_3^- uptake and N_2 gas suggesting direct denitrification, but this relationship was not found at Elders East. These patterns are supported by the higher SOD at Elders East (Figure 9) which could be due to greater nitrification, while sediments with a lower SOD such as those Black Bank would be more likely to be supported by direct denitrification.

Uptake of NO_x^- in both sites in this study were higher than uptake rates reported in a previous study at a neighboring Jamaica Bay marsh known as Yellow Bar (Zhu et al. 2019). For example, NO_x^- uptake at Black Bank was comparable to levels reported by Zhu et al. (2019), but uptake at Elders East was ~0.5 times higher than both Black Bank and Yellow Bar values from this study despite similar water column NO_x^- and in

the study by Zhu et al. (2019). Elders East also had correspondingly higher levels of N_2 production. At Yellow Bar, carbon availability appeared to be an important driver of denitrification; however, sediment carbon was much higher at Black Bank than Elders East. In this case it may be possible that carbon and reduced sediment conditions at Black Bank were inhibiting denitrification.

It is likely that the *Ulva* blooms and diel hypoxia contributed to reduced sediment conditions which modified N transformations at these study sites. Hypoxia often corresponds with elevated production of H_2S, a by-product of organic matter decomposition (An and Gardner 2002; Rysgaard et al. 1996; Alldred et al. 2020) that is known to inhibit both nitrification and denitrification (Gould and McCready 1982; Jensen and Cox 1992; Joye and Hollibaugh 1995). The high H_2S levels have been described to occur following peaks in *Ulva* biomass, with the greatest concentrations found beneath mats of decaying *Ulva* (Senga et al. 2021). In Jamaica Bay, *Ulva* biomass declines in Fall (Lamb 2018) which is also when sediment cores for nutrient and gas flux measurements were collected. Alldred et al. (2020) found O_2 extinction depth to be shallowest in Fall and Black Bank marsh generally had the lower O_2 and higher sulfide concentrations than Elders East. Therefore, denitrification may have been higher at Elders East because of less sulfide inhibition, although sulfide was not measured at the time of sampling. Future studies should include sulfide measurements to inform a mechanistic understanding of denitrification in urban eutrophic salt marshes (Bernard et al. 2015).

The total N mineralization rates (i.e., DIN fluxes + N_2 fluxes) were higher at Elders East than Black Bank due to the greater denitrification and NH_4^+ effluxes at

Elders East. Nitrification is generally limited by O_2 and NH_4^+, but both sites had positive fluxes of NH_4^+ which indicates neither were limited by NH_4^+. The evidence suggests that Black Bank was more reduced, and nitrification was more limited there and thus had lower denitrification. The NH_4^+ efflux at Elders East, however, was more than twofold higher than Black Bank. This could be due to greater rates of ammonification as the sandy sediments were more oxygenated and supported greater O_2 uptake. Alternatively, the NH_4^+ effluxes could be partially attributed to dissimilatory nitrate reduction to ammonium (DNRA). The quantity of NO_x^- that was assimilated by the sediment exceeded the amount of N_2 produced. Thus, there was a significant amount of NO_x^- assimilated but unaccounted for through denitrification. The NO_x^- could have been reduced through DNRA. Several factors have been positively related to DNRA including sulfide concentrations (Gardner et al. 2006; Plummer et al. 2015), quantity and quality of organic carbon (Christensen et al. 2003; Murphy et al. 2016), and the ratio of organic carbon to nitrate (Hardison et al. 2015). At the study sites, Black Bank had higher organic carbon (Table 1), greater sulfide (Alldred et al. 2020), and since both sites had the same NO_3^-, Black Bank had higher ratio of organic C to NO_3^-. These conditions would indicate greater potential for DNRA at Black Bank, yet, higher NH_4^+ effluxes were observed at Elders East. In addition, Lindemann et al. (2016) found much lower abundance of the genes responsible for DNRA (e.g., *nfrA*) as compared to those responsible for denitrification (e.g. *nirS, nirK*). Therefore, it can be concluded that the high NH_4^+ effluxes were largely due to rapid mineralization of organic matter (i.e., *Ulva* and microalgae). Lastly, it is also possible that *Ulva* accumulation on sediments may have contributed to incomplete denitrification, which

is the release of the greenhouse gas N_2O instead of completing the denitrification process to N_2 (Wong et al. 2021), but N_2O production was not measured.

Ulva *blooms, acidification, and their ecosystem impacts*

Large blooms of macroalgae can have significant impacts on ecosystem health (Glibert 2020). The results of the current study corroborate previous studies (Wallace et al. 2014) and demonstrate how *Ulva* beds can alter oxygen and pH dynamics in eutrophic coastal ecosystems. Significant diel fluxes of O_2 and pH were observed during summer when respiration was highest and speculate that pH slowly declined in late summer when the *Ulva* started to decay. Interestingly, no effect of acidification on sediment N processes was found but it is believed that the presence of *Ulva* impacted N transformations at the study sites. Lamb (2018) reported a doubling of water column NO_x^- concurrent with low September *Ulva* biomass. Similar increases of NO_x^- concurrent with *Ulva* declines were shown by Malta and Vershuure (1997) and Malta et al. (2002). Furthermore, Lamb's study reported DIN concentrations were highest in September and June, at ~1.0 mg L^{-1} which was comparable to the DIN concentration found in inflow header tanks during core incubations (a DIN concentration of 0.91 mg L^{-1}). This is consistent with other studies of water chemistry in Jamaica Bay (Hoellein and Zarnoch 2014; Lindemann et al. 2016). This suggests greater potential for denitrification when *Ulva* biomass is reduced and denitrifiers are not competing for water column NO_3^-. However, it was found that denitrification was supported through coupled nitrification-denitrification at Elders East (sandy, aerobic sediment) and was limited at Black Bank due to reduced sediment conditions. It is quite possible that *Ulva*

biomass contributed to both the organic matter mineralization supporting nitrification at Elders East and the buildup of sulfide at Black Bank, demonstrating the connections between carbon and nitrogen cycling at these sites.

In the teabag experiment, it had been hypothesized that the addition of labile carbon to recalcitrant carbon would enhance decomposition of the recalcitrant carbon and found that there was no effect of cometabolism. However, a greater decomposition rate of recalcitrant material was seen at Black Bank marsh. This could have negative implications for marsh health as Black Bank is a degrading marsh and appears to lose recalcitrant carbon faster than a restored marsh. *Ulva* biomass accumulation at Black Bank likely contributes to the sulfidic and anaerobic conditions that promote marsh degradation and carbon loss. It would be valuable to have future studies consider both the direct and indirect processes in which macroalgal blooms can impact critical ecosystem services such as nitrogen removal and carbon sequestration in coastal ecosystems.

ACKNOWLEDGMENTS

I wish to thank my advisor, Dr. Chester Zarnoch, and the chair of my doctoral advisory committee, Dr. J. Stephen Gosnell, for their invaluable assistance on this project and paper. I also would like to thank Thomas Whaley, Ahmed Abbas, Caroline Troy, Lauryn Tham, and Ivette Evangelista with their help in the lab and field.

REFERENCES

Alldred, M., J.J. Borrelli, T. Hoellein, D. Bruesewitz , and C. Zarnoch. 2020. Marsh plants enhance coastal marsh resilience by changing sediment oxygen and sulfide concentrations in an urban, eutrophic estuary. Estuaries and Coasts 43:801–813.

Alldred, M., A. Liberti, and S.B. Baines. 2017. Impact of salinity and nutrients on salt marsh stability. Ecosphere 8: p.e02010.

An, S., and W.S. Gardner. 2002. Dissimilatory nitrate reduction to ammonium (DNRA) as a nitrogen link, versus denitrification as a sink in a shallow estuary (Laguna Madre/Baffin Bay, Texas). Marine Ecology Progress Series 237:41–50.

APHA. 1998. Standard methods for the examination of water and wastewater, 20th ed. United Book Press, Inc, Baltimore.

Bates, D.M. 2010. Lme4: mixed-effects modeling with R. http:// lme4.r-forge.r-project.org/book/

Bates, D., M. Maechler, B. Bolker, and S. Walker. 2015. Fitting Linear Mixed-Effects Models Using lme4. Journal of Statistical Software 67:1-48.

Beman, J.M., C.E. Chow, A.L. King, Y. Feng, J.A. Fuhrman, A. Andersson, N.R. Bates, B.N. Popp, and D.A. Hutchins. 2011. Global declines in oceanic nitrification rates as a consequence of ocean acidification. Proceedings of the National Academy of Sciences 108:208–13.

Benfield, E.F., 2006. Decomposition of leaf material. pp. 711–720 In: Hauer, F.R., and G.A. Lamberti (Eds.), Methods in Stream Ecology. Academic Press, San Diego, CA.

Bernard, R.J., B. Mortazavi, and A.A. Kleinhuizen. 2015. Dissimilatory nitrate reduction to ammonium (DNRA) seasonally dominates NO_3^- reduction pathways in an anthropogenically impacted sub-tropical coastal lagoon. Biogeochemistry 125:47–64.

Bernhard, A.E., Z.C. Landry, A. Blevins, J.R. de la Torre, A.E. Giblin, and D.A. Stahl. 2010. Abundance of ammonia-oxidizing archaea and bacteria along an estuarine salinity gradient in relation to potential nitrification rates. Applied and Environmental Microbiology 76:1285-1289.

Boynton, W.R. and W.M. Kemp. 1985. Nutrient regeneration and oxygen consumption by sediments along an estuarine salinity gradient. Marine Ecology Progress Series, 23:45-55.

Brigolin, D., C. Rabouille, C. Demasy, B. Bombled, G. Monvoisin, and R. Pastres. 2021. Early diagenesis in sediments of the Venice Lagoon (Italy) and its relationship to hypoxia. Frontiers in Marine Science 7:1039.

Campbell, A., Y. Wang, M. Christiano, and S. Stevens. 2017. Salt marsh monitoring in Jamaica Bay, New York from 2003 to 2013: a decade of change from restoration to Hurricane Sandy. Remote Sensing 9:131.

Christensen, P.B., R.N. Glud, T. Dalsgaard, and P. Gillespie. 2003. Impacts of longline mussel farming on oxygen and nitrogen dynamics and biological communities of coastal sediments. Aquaculture 218:567–88.

Coffaro, G., and A. Sfriso. 1997. Simulation model of *Ulva rigida* growth in shallow water of the Lagoon of Venice. Ecological Modelling, Development of Models with Dynamic Structure for Marine Ecosystems 102:55–66.

Craft, C., P. Megonigal, S. Broome, J. Stevenson, R. Freese, J. Cornell, L. Zheng, and J. Sacco. 2003. The pace of ecosystem development of constructed *Spartina alterniflora* marshes. Ecological Applications 13:1417-1432.

Day, J.W., R.D. DeLaune, J.R. White, R.R. Lane, R.G. Hunter, and G.P. Shaffer. 2018. Can denitrification explain coastal wetland loss: A review of case studies in the Mississippi Delta and New England. Estuarine, Coastal and Shelf Science 213: 294–304.

Deegan, L.A., D.S. Johnson, R.S. Warren, B.J. Peterson, J.W. Fleeger, S. Fagherazzi, and W.M. Wollheim. 2012. Coastal eutrophication as a driver of salt marsh loss. Nature 490:388–392.

Fox, J., and H.S. Weisberg. 2011. An R companion to applied regression, SAGE Publications, Thousand Oaks, CA. 2nd Edition.

Fulweiler, R.W., H.E. Emery, E.M. Heiss, and V.M. Berounsky. 2011. Assessing the role of pH in determining water column nitrification rates in a coastal system. Estuaries and Coasts 34:1095-1102.

Galloway, J.N., J.D. Aber, J.W. Erisman, S.P. Seitzinger, R.W. Howarth, E.B. Cowling, and B.J. Cosby. 2003. The nitrogen cascade. Bioscience 53:341-356.

Gardner, W.S., M.J. McCarthy, S. An, D. Sobolev, K.S. Sell, and D. Brock. 2006. Nitrogen fixation and dissimilatory nitrate reduction to ammonium (DNRA) support nitrogen dynamics in Texas estuaries. Limnology and Oceanography 51: 558–568.

Gazeau, F., P. van Rijswijk, L. Pozzato, and J.J. Middelburg. 2014. Impacts of ocean acidification on sediment processes in shallow waters of the Arctic Ocean. PLOS ONE 9: e94068.

Giblin, A.E., C.R. Tobias, B. Song, N. Weston, G.T. Banta, and H. Rivera-Monroy, V. 2013. The importance of dissimilatory nitrate reduction to ammonium (DNRA) in the nitrogen cycle of coastal ecosystems. Oceanography 26:124-131.

Glibert, P.M. 2020. Harmful algae at the complex nexus of eutrophication and climate change.. Harmful Algae 91:101583.

Gobler, C.J., and W.G. Sunda. 2012. Ecosystem disruptive algal blooms of the brown tide species, *Aureococcus anophagefferens* and *Aureoumbra Lagunensis.* Harmful Algae 14:36–45.

Gould, W.D., G.L McCready. 1982. Denitrification in several soils: inhibition by sulfur anions. Canadian Journal of Microbiology 28:334–340.

Gruber, R.K., R.J. Lowe, and J.L. Falter. 2017. Metabolism of a tide-dominated reef platform subject to extreme diel temperature and oxygen variations. Limnology and Oceanography 62:1701–1717.

Hamersley, M.R., B.L. Howes. 2005. Coupled nitrification/denitrification measured in situ in a *Spartina alterniflora* marsh with a 15NH4+ tracer. Marine Ecology Progress Series 299:123−135.

Hardison, A.K., C.K. Algar, A.E. Giblin, and J.J. Rich. 2015. Influence of organic carbon and nitrate loading on partitioning between dissimilatory nitrate reduction to ammonium (DNRA) and N2 production. Geochimica et Cosmochimica Acta 164: 146–160.

Haro, S., J. Bohórquez, M. Lara, E. Garcia-Robledo, C.J. González, J.M. Crespo, S. Papaspyrou, and A. Corzo. 2019. Diel patterns of microphytobenthic primary production in intertidal sediments: the role of photoperiod on the vertical vigration circadian rhythm. Scientific Reports 9:13376.

Hartig, E.K., V. Gornitz, A. Kolker, F. Mushacke, and D. Fallon. 2002. Anthropogenic and climate-change impacts on salt marshes of Jamaica Bay, New York City. Wetlands 22:71-89.

Hoellein, T.J., and C.B. Zarnoch. 2014. Effect of Eastern oysters (*Crassostrea virginica*) on sediment carbon and nitrogen dynamics in an urban estuary. Ecological Applications 24:271–86.

Hothorn, T.; F. Bretz, and P. Westfall. 2008. Simultaneous inference in general parametric models. Biometrical Journal 50:346-363.

Howarth, R.W. and R. Marino. 2006. Nitrogen as the limiting nutrient for eutrophication in coastal marine ecosystems: Evolving views over three decades. Limnology and Oceanography 51:364-376.

Hutchins, D.A., M.R. Mulholland, and F. Fu. 2009. Nutrient cycles and marine microbes in a CO_2-enriched ocean. Oceanography 22:128–145.

Hutchins, D.A., and F. Fu. 2017. Microorganisms and ocean global change. Nature Microbiology 2:1–11.

Jensen, K.M., and R.P. Cox. 1992. Effects of sulfide and low redox potential on the inhibition of nitrous oxide reduction by acetylene in *Pseudomonas nautica*. FEMS Microbiology Letters 96:13–18.

Joye, S.B., and J.T. Hollibaugh. 1995. Sulfide inhibition of nitrification influences nitrogen regeneration in sediments. Science 270:623–625.

Kana, T.M., C. Darkangelo, M.D. Hunt, J.B. Oldham, G.E. Bennett, and J.C. Cornwell. 1994. Membrane inlet mass spectrometer for rapid high-precision determination of N2, O2, and Ar in environmental water samples. Analytical Chemistry 66:4166–4170.

Keuskamp, J.A., B.J.J. Dingemans, T. Lehtinen, J.M. Sarneel, and M.M. Hefting. 2013. Tea Bag Index: A novel approach to collect uniform decomposition data across ecosystems. Methods in Ecology and Evolution 4:1070–1075.

Kitheka, J.U., B.O. Ohowa, B.M. Mwashote, W.S. Shimbira, J.M. Mwaluma, and J. M. Kazungu. 1996. Water circulation dynamics, water column nutrients and plankton productivity in a well-flushed tropical bay in Kenya. Journal of Sea Research 35:257–268.

Kitidis, V., B. Laverock, L.C. McNeill, A. Beesley, D. Cummings, K. Tait, M.A. Osborn, and S. Widdicombe. 2011. Impact of ocean acidification on benthic and water column ammonia oxidation. Geophysical Research Letters 38: 21.

Koop-Jakobsen K., and A.E. Giblin. 2010. The effect of increased nitrate loading on nitrate reduction via denitrification and DNRA in salt marsh sediments. Limnology and Oceanography 55:789−802.

Lamb, A. 2018. *Ulva* spp. bloom dynamics in a hyper-eutrophic estuary: Jamaica Bay, New York. Doctoral Dissertation. The Graduate Center, City University of New York, New York.

Lindemann, S., C.B. Zarnoch, D. Castignetti, and T.J. Hoellein. 2016. Effect of Eastern oysters (*Crassostrea virginica*) and seasonality on nitrite reductase gene abundance (NirS, NirK, NrfA) in an urban estuary. Estuaries and Coasts 39:218–232.

Liu, S., S.M. Trevathan-Tackett, C.J. Ewers Lewis, X. Huang, and P.I. Macreadie. 2020. Macroalgal blooms trigger the breakdown of seagrass blue carbon. Environmental Science & Technology 54:14750–14760.

Lowell, A., E. Infantes, L. West, L.Puishys, C.E. L. Hill, K. Ramesh, B. Peterson, J. Cebrian, S. Dupont, and T.E. Cox. 2021. How does ocean acidification affect the early life history of *Zostera marina*? A series of experiments find parental carryover can benefit viability or germination. Frontiers in Marine Science 8.

Malta, E., J.M. Verschuure, and P.H. Nienhuis. 2002. Regulation of spatial and seasonal variation of macroalgal biomass in a brackish, eutrophic lake. Helgoland Marine Research 56:211–20.

Malta, E.J. and J.M. Verschuure. 1997. Effects of environmental variables on between-year variation of *Ulva* growth and biomass in a eutrophic brackish lake. Journal of Sea Research 38:71–84.

Marley, A.R.G., C. Smeaton, and W.E.N. Austin. 2019. An assessment of the Tea Bag Index method as a proxy for organic matter decomposition in intertidal environments. Journal of Geophysical Research: Biogeosciences 124:2991–3004.

McCarthy, M., P. Lavrentyev, L. Yang, L. Zhang, Y. Chen, B. Qin, and W. Gardner. 2007. Nitrogen dynamics and microbial food web structure during a summer cyanobacterial bloom in a subtropical, shallow, well-mixed, eutrophic lake (Lake Taihu, China). pp. 195–207 In: Qin, B., Liu, Z., Havens, K. (Eds.), Eutrophication of Shallow Lakes with Special Reference to Lake Taihu, China. Springer, Dordrecht.

Mozdzer, T.J., S.E. Drew, J.S. Caplan, P.E. Weber, and L.A. Deegan. 2021. Rapid recovery of carbon cycle processes after the cessation of chronic nutrient enrichment. Science of The Total Environment 750:140927.

Mueller, P., L.M. Schile-Beers, T.J. Mozdzer, G.L. Chmura, T. Dinter, Y. Kuzyakov, A.V. de Groot, P. Esselink, C. Smit, A. D'Alpaos, C. Ibáñez, M. Lazarus, U. Neumeier, B.J. Johnson, A.H. Baldwin, S.A. Yarwood, D.I. Montemayor, Z. Yang, J. Wu, K. Jensen, and S. Nolte. 2018. Global-change effects on early-stage decomposition processes in tidal wetlands – implications from a global survey using standardized litter. Biogeosciences 15:3189–3202.

Murphy, A.E., I.C. Anderson, A.R. Smyth, B. Song, and M.W. Luckenbach. 2016. Microbial nitrogen processing in hard clam (*Mercenaria mercenaria*) aquaculture sediments: the relative importance of denitrification and dissimilatory nitrate reduction to ammonium (DNRA). Limnology and Oceanography 61:1589-1604.

Murphy, J. and J. Riley. 1962. A modified single solution method for the determination of phosphate in natural waters. Analytica Chimica Acta 27:31–36.

National Oceanic and Atmospheric Administration (NOAA). 2021. Annual Prediction Tide Tables, Beach Channel, NY (Report no. 8517137).

Newton, C., and C. Thornber. 2012. Abundance and Species Composition Surveys of Macroalgal Blooms in Rhode Island Salt Marshes. Northeastern Naturalist 19: 501–516.

New York City Department of Environmental Protection (NYCDEP). 1996. Harbor Survey Report, New York.

New York City Department of Parks and Recreation (NYC Parks). 2012. New York City Wetlands Strategy. NYC Parks. http://www.nyc.gov/html/planyc2030/downloads/pdf/nyc_wetlands_strategy.pdf.

Nieuwenhuize, J., Y.E.M. Maas, and J.J. Middelburg. 1994. Rapid analysis of organic carbon and nitrogen in particulate materials. Marine Chemistry 45:217–224.

Piehler, M.F., and A.R. Smyth. 2011. Habitat-specific distinctions in estuarine denitrification affect both ecosystem function and services. Ecosphere 2:1–17.

Plummer, P., C. Tobias, and D. Cady. 2015. Nitrogen reduction pathways in estuarine sediments: influences of organic carbon and sulfide. Journal of Geophysical Research: Biogeosciences 120:1958–1972.

Rabalais, N.N., R.E. Turner, and W.J. Wiseman. 2002. Gulf of Mexico hypoxia, a.k.a. "The Dead Zone." Annual Review of Ecology and Systematics 33: 235–63.

Radabaugh, K.R., R.P. Moyer, A.R. Chappel, C.E. Powell, I. Bociu, B.C. Clark, and J.M. Smoak. 2018. Coastal blue carbon assessment of mangroves, salt marshes, and salt barrens in Tampa Bay, Florida, USA. Estuaries and Coasts 41:1496–1510.

Rosenzweig, B.R., P.M. Groffman, C.B. Zarnoch, B.F. Branco, E.K. Hartig, J. Fitzpatrick, H.M. Forgione, and A. Parris. 2018. Nitrogen regulation by natural systems in "unnatural" landscapes: denitrification in ultra-urban coastal ecosystems. Ecosystem Health and Sustainability 4:205-224.

Rysgaard, S., N. Risgaard-Petersen, and N. Sloth. 1996. Nitrification, denitrification and nitrate ammonification in two coastal lagoons in Southern France. Hydrobiologia 329:133-141.

Seelen, L.M.S., G. Flaim, J. Keuskamp, S. Teurlincx, R. Arias Font, D. Tolunay, M. Fránková, K. Sumberová, M. Temponeras, M. Lenhardt, E. Jennings, L.N. de Senerpont Domis. 2019. An affordable and reliable assessment of aquatic decomposition: tailoring the Tea Bag Index to surface waters. Water Research 151:31–43.

Seitzinger, S., J.A. Harrison, J.K. Böhlke, A.F. Bouwman, R. Lowrance, B. Peterson, C. Tobias, and G. Van Drecht. 2006. Denitrification Across Landscapes and Waterscapes: A Synthesis. Ecological Applications 16:2064–2090.

Senga, Y., W. Kobayashi, K. Mikawa, T. Kitazawa, S. Lee, and Y. Shiraki. 2021. Influences of green macroalgae blooms on nutrients and sulfide dynamics in hypereutrophic intertidal ecosystems. Limnology 22:187–96.

Shaha, D.C., Y.-K. Cho, G.-H. Seo, C.-S. Kim, and K.T. Jung. 2010. Using flushing rate to investigate spring-neap and spatial variations of gravitational circulation and tidal exchanges in an estuary. Hydrology and Earth System Sciences 14:1465–1476.

Solorzano, L. 1969. Determination of ammonium in natural waters by the phenolhypochlorite method. Limnology and Oceanography 14:799–801.

Tomasetti, S.J., J.R. Kraemer, and C.J. Gobler. 2021. Brief episodes of nocturnal hypoxia and acidification reduce survival of economically important blue crab (*Callinectes sapidus*) larvae. Frontiers in Marine Science 8:1190.

Valiela, I., J. McClelland, J. Hauxwell, P.J. Behr, D.Hersh, and K. Foreman. 1997. Macroalgal blooms in shallow estuaries: controls and ecophysiological and ecosystem consequences. Limnology and Oceanography 42:1105–18.

Vieillard, A.M., and R.W. Fulweiler. 2012. Impacts of long-term fertilization on salt marsh tidal creek benthic nutrient and N2 gas fluxes. Marine Ecology Progress Series 471:11–22.

Wallace, R.B., H. Baumann, J.S. Grear, R.C. Aller, and C.J. Gobler. 2014. Coastal ocean acidification: The other eutrophication problem. Estuarine, Coastal and Shelf Science 148:1–13.

Wallace, R.B., and C.J. Gobler. 2015. Factors controlling blooms of microalgae and macroalgae (*Ulva rigida*) in a eutrophic, urban estuary: Jamaica Bay, NY, USA. Estuaries and Coasts 38:519–33.

Webb, K.L., and C.F. D'Elia. 1980. Nutrient and oxygen redistribution during a spring neap tidal cycle in a temperature estuary. Science 207:983–85.

Whitfield, A.K. 1988. The role of tides in redistributing macrodetrital aggregates within the Swartvlei Estuary. Estuaries 11:152–59.

Wickham, H. 2016. ggplot2: Elegant Graphics for Data Analysis. Springer-Verlag. New York.

Wigand, C., C.T. Roman, E. Davey, M. Stolt., R. Johnson, A. Hanson, E.B. Watson, S.B. Moran, D.R. Cahoon, J.C. Lynch, and P. Rafferty. 2014. Below the disappearing marshes of an urban estuary: historic nitrogen trends and soil structure. Ecological Applications 24.4:633-649.

Wong, W.W., C. Greening, G. Shelley, R. Lappan, P.M. Leung, A. Kessler, B. Winfrey, S.C. Poh, and P. Cook. 2021. Effects of drift algae accumulation and nitrate loading on nitrogen cycling in a eutrophic coastal sediment. Science of The Total Environment 790:147749.

Yao, H., Y. Gao, G.W. Nicol, C.D. Campbell, J.I. Prosser, L. Zhang, W. Han, and B.K. Singh. 2011. Links between ammonia oxidizer community structure, abundance, and nitrification potential in acidic soils. Applied and Environmental Microbiology 77:4618-4625.

Zarnoch, C.B., T.J. Hoellein, B.T. Furman, and B.J. Peterson. 2017. Eelgrass meadows, *Zostera marina* (L.), facilitate the ecosystem service of nitrogen removal during simulated nutrient pulses in Shinnecock Bay, New York, USA. Marine Pollution Bulletin 124:376–87.

Zhu, J., C. Zarnoch, J.S. Gosnell, M. Alldred, and T. Hoellein. 2019. Ribbed mussels *Geukensia demissa* enhance nitrogen-removal services but not plant growth in restored eutrophic salt marshes. Marine Ecology Progress Series 631:67–80.

Zuur A.F. 2009. Mixed effects models and extensions in ecology with R. Springer, New York, NY.